SLAM CHARACTERISTICS OF A HIGH-SPEED WAVE PIERCING CATAMARAN IN IRREGULAR WAVES

(DOI No: 10.3940/rina.ijme.2014.a1.274)

B J French and **G A Thomas**, Australian Maritime College, University of Tasmania, Australia and **M R Davis,** University of Tasmania, Australia

SUMMARY

Slam characteristics of a 112m INCAT wave piercing catamaran in a range of realistic irregular sea conditions are presented in this paper. Towing tank testing of a 2.5 m hydroelastic segmented catamaran model was used to gather a database of slam events in irregular seas. The model was instrumented to measure motions, centrebow surface pressures and forces, encountered wave elevations and wave elevations within the bow area tunnel arches. From these measurements characteristics of the vessel slamming behaviour are examined: in particular relative vertical velocity, centrebow immersion, archway wave elevations and slam load distributions. A total of 2,098 slam events were identified over 22 different conditions, each containing about 80 to 100 slam events.

The data, although inherently scattered, shows that encounter wave frequency and significant wave height are important parameters with regard to centrebow slamming. Relative vertical velocity was found to be a poor indicator of slam magnitude and slams were found to occur before the centrebow arch tunnel was completely filled, supporting the application of a two-dimensional filling height parameter as a slam indicator.

NOMENCLATURE

λ	Wave length (m)
ω_e	Encountered angular frequency (rad s^{-1})
ω_e^*	Dimensionless encountered angular frequency
c	Wave celerity (m s^{-1})
d	Water depth (m)
f_e	Encountered wave frequency (Hz)
g	Gravitational constant (m s^{-2})
$H_{1/3}$	Significant wave height (m)
L	Vessel length (m)
r	Correlation coefficient
T_0	Wave modal period (s)
U	Vessel speed (m s^{-1})

1. INTRODUCTION

Large fast aluminium catamarans vehicle ferries have been developed over the past two decades. Originally designed to operate in sheltered waters, conventional catamaran ferries were commonly constructed with a small wetdeck clearance [1]. If such vessels are exposed to significant seas, not only does passenger discomfort increase but the increased motions of the vessel leads to wave impacts on the relatively low wetdeck structure.

In an effort to reduce vessel motions in unsheltered waters, the wave piercing hull form was developed. In this design the hull flare above the water line is completely removed in the bow area. This wave piercing hull form was successful in reducing motions. However, wave piercing vessels can become susceptible to deep bow entry due to insufficient reserve buoyancy at the bow. To combat this tendency, the high-speed aluminium catamaran manufacturer, INCAT Tasmania, developed the centrebow hull form, which is in essence a short bow-mounted third hull located on the cross deck structure between the wave piercing demihulls. The centrebow is designed such that its keel rests close to the calm water line so that in calm or mild sea conditions the centrebow is out of the water for the majority of wave encounters, resulting in small centrebow loads. In larger seas, however, the centrebow acts to provide reserve buoyancy to prevent bow entry into encountered waves. If the bow enters deeply into the water, the archways between the centrebow and demihulls can completely fill, resulting in large slam forces [1].

Previous scale model experiments into the slam characteristics of high speed wave piercing catamarans have concentrated on regular waves [2, 3]. Preliminary tests in irregular seas have been conducted [4], however a larger set of tests are required to gain more confidence in the characteristics of slam in irregular seas. This work further expands irregular sea research by investigating the slam characteristics of a 112m INCAT catamaran in a range of realistic irregular sea conditions through the use of scale model towing tank testing. In particular relative vertical velocity, centrebow immersion, archway wave elevations and slam load are experimentally measured and investigated. Due to the unrepeatable nature of irregular sea tests, the distributions of these parameters are investigated.

2. HYDROELASTIC SEGMENTED MODEL

A 2.5 m hydroelastic segmented catamaran model, representative of the 112m INCAT wave-piercing catamaran was used for these tests (the vessel particulars are shown in Table 1). The model was designed such that the main whipping vibration mode frequency was correctly scaled to full scale. Since the full scale vessel was not built at the design stage of the model, the target whipping frequency of the model was based on a FE modal analysis of the full scale 112m vessel. The full scale vessel was expected to have a whipping frequency of 13.8 Hz, equating to 2.4 Hz at model scale [5]. The desired whipping frequency was achieved by controlling the dimension (and thus stiffness) of the aluminium elastic links joining the demihull segments.

The model was constructed from carbon fibre and Divinycell foam sandwich to obtain a light-weight yet high hull segment stiffness. Each demihull of the model was separated into three segments (see Figure 1) and joined together with elastic aluminium links. Each segment was stiffened with aluminium 40mm hollow square section backbone beam, into which the elastic links fitted. The advantage of using solid aluminium links is that they can be shaped to the dimensions required to model the frequency of the main bending mode, and can be interchanged with links of different dimensions and thus stiffnesses. Strain gauges were mounted on the elastic links, allowing the measurement of demihull bending moments.

Table 1: Main particulars of the 2.5m hydroelastic segmented catamaran.

	Model Scale	Full Scale
Scale	1:44.8	1:1
Displacement	30 kg	2,764 tonnes
Trim	Level	
Radius of gyration in pitch	640 mm (25.6%L)	
Trim tab angle	7 degrees	
Centrebow truncation from transom	1902 mm	85.2 m
LCG from transom	954 mm	42.7 m
Centrebow truncation to LCG	948 mm	42.5 m
Max. arch height from undisturbed CWL	76.4 mm	3.4 m

The centrebow segment was isolated from the demihulls and supported by two aluminium transverse beams. The beams were pin-joined to the forward demihull segments (shown in Figure 1) and elastic links with attached strain gauges within the transverse beams were used to determine the magnitudes of vertical loads on the centrebow and their locations.

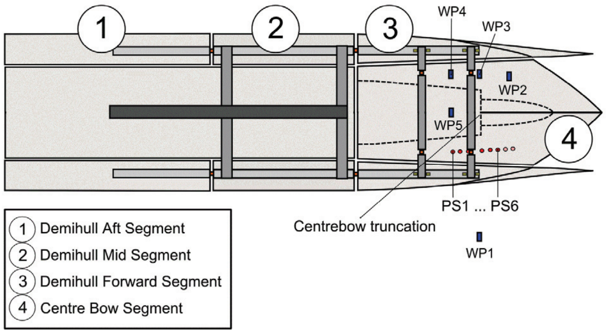

Figure 1: Diagram showing the model layout and locations of the pressure transducers. The demihull segments and centrebow segment are also labelled and shown.

Two different centrebow segments were constructed: a standard one and one containing 84 pressure tappings over the starboard arch extending from frame 55 to frame 82 with reference to the full scale vessel. Since the bow containing the pressure tappings is substantially heavier than the standard bow, the centrebows can be interchanged when pressure measurements are not desired. Centrebow surface pressures were measured during these tests and therefore the heavier pressure tapped bow was installed. This meant that in order to meet trim and radius of gyration requirements the displacement of the model was raised to 30 kg, representing a full scale displacement of 2,764 tonnes which is a realistic part overload condition. This vessel has a maximum 500 tonne deadweight overload with a displacement of 3000 tonnes when it operates at somewhat reduced speed compared to the nominal design displacement of 2500 tonnes.. The vessel is of course more exposed to slamming in the overload conditions.

3. INSTRUMENTATION AND TEST CONDITIONS

The towing tank at the Australian Maritime College was used to create the test environment for the model. The tank is 100 m long and 3.55 m wide, with a maximum depth of 1.5 m. A paddle type wave maker, capable of producing irregular wave spectra is located at the far end of the tank. In order to reduce reflections from the wave maker, a large beach is located at the opposite end of the tank and pneumatically retractable beaches are installed along the length of the tank so as to smooth the water more rapidly between test runs. A towing carriage is mounted on rails above the tank and is free to traverse the entire length of the tank. The velocity of the carriage can be varied up to a maximum of 4.6 m/s. The carriage carries its own on-board DAQ and signal conditioning systems with the capacity to record up to 16 channels.

The blockage ratio for the hydroelastic catamaran model in the AMC facility was determined to be 0.0045; therefore no blockage corrections were required for the model speeds tested.

The model was extensively instrumented with linear variable differential transducers (LVDTs), wave probes mounted both on the model itself and alongside, strain gauges located on the demihull and centrebow segments to measure vertical bending moments and centrebow slam loads respectively and pressure sensors located on the centrebow segment archway.

The vertical motion of the model was measured at each of the two tow posts using LVDTs. This provided data to calculate model heave and pitch motions as well as vertical acceleration.

Five resistance/capacitance type (one mounted on a foil) wave probes were used during testing. The wave probes consist of two steel probes that are partway inserted into

the water. The resistance across the probes varies linearly with the amount of submersion of the probes. The foil-mounted capacitance wave probe (WP1 in Figure 1) was fixed to the carriage in the plane of the centrebow truncation and offset to one side of the model by 0.8 m.
The four other probes were shortened and installed on the bow segment of the model (as shown in Figure 1). The probes protruded 140 mm from the surface of the wet deck, perpendicular to the calm water line, as shown in Figure 2. Three probes were mounted on the port side of the centrebow longitudinally along the maximum arch height, WP3 (with reference to Figure 1) in the plane of the centrebow truncation. WP2 was 120 mm forward of WP3 and WP4 120 mm aft of WP3. The fifth wave probe (WP5) was mounted on the centerline of the model, aft of the centrebow truncation in the plane of the port wave probe furthest aft (WP4). Figure 2 is a photo of the underside of the model, showing the four shortened boat mounted wave probes. The centrebow is visible in the top section of this photo, as well as the yellow latex and waterproof tape used to seal the segment gaps.

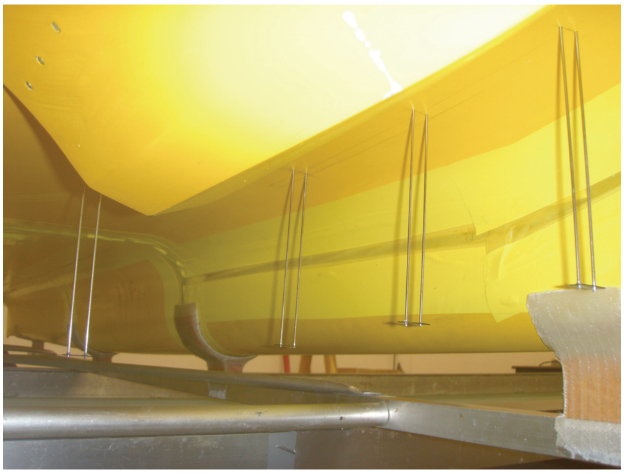

Figure 2: View looking aft and towards the port underside of the model showing the four hull mounted wave probes (from left to right WP5, WP4, WP3 and WP2). Three pressure tappings can be seen on the centrebow in the top left corner. Also visible in this photo are the centrebow truncation and sealing of the segment gaps with flexible latex sheet and adhesive yellow tapes.

Six pressure transducers were installed on the model, along the top of the archway (Endevco model 8510C-50). During testing in large wave heights the largest pressures were measured further forward on the archway. Therefore the two furthest aft transducers were moved to the forward positions when testing in these sea states (PS1 and PS2 were moved to the positions highlighted by the unfilled circles shown in Figure 1).

The project team had previously conducted two-dimensional drop tests of wave piercing catamaran style centrebows and the maximum measured pressures were found to be in the range of 170 kPa [6]. When these loads are scaled to full scale they exceeded the largest measured slams by a factor of approximately three [7]. The maximum drop test loads were determined by measuring the maximum accelerations during water entry. The full scale slam load per unit length was calculated from full scale trials strain gauge records and a quasi-static finite element analysis [7]. Therefore the comparison was based on maximum peak values. It is expected that three dimensional effects present in scale model seakeeping tests would reduce the maximum measured slam pressures to less than that of the two-dimensional drop tests.

3.1 TEST CONDITIONS

Slam events in irregular seas are inherently varied. Therefore in order to investigate the characteristics of these events, a sufficiently large number of events need to be observed. As with any statistical process, more sample observations lead to a greater confidence in the underlying parameter distributions. Therefore the number of conditions and time spent testing each must be balanced. One approach to this problem is to record hundreds of slams in a single sea condition, thus gaining a thorough understanding of the slam behaviour in that particular condition, neglecting the influence of environmental parameters such as the effect of significant wave height on slam occurrences and severity. The other approach, and the one adopted for this study, is to estimate the number of slam events required to illustrate the underlying parameter distribution and then develop a test matrix and investigate the influence of sea state on the vessel slam characteristics.

Table 2: Test parameters.

	Modal Period (s)	Significant Wave Height	Ship Speed
Model Scale	1 1.3 1.5	55.8 mm 67.0 mm 78.1 mm 89.3 mm	1.53 m/s 2.15 m/s 2.92 m/s
Full Scale	7 8.5 10	2.5 m 3.0 m 3.5 m 4.0 m	20 knots 28 knots 38 knots

In order to determine ship motion behaviour in irregular seas, Lloyd [8] recommends that at least 100 pairs of peaks and troughs should be encountered. Since slams do not occur on every wave encounter, it was decided to encounter at least 300 waves per condition. This equated to roughly eight runs in the towing tank per condition. Given the time allocated in the towing tank and the required eight runs per condition, a test matrix of 22 test conditions were selected. At full scale three different vessel speeds (20, 28 and 38 knots), three modal periods (7, 8.5 and 10 s) and two significant wave heights (2.5, 3.0, 3.5 and 4.0 m) formed the core of the test matrix. The influence of wave height on the slamming behaviour was of particular interest. Due to time constraints, two additional wave heights (2.5 and 3.0 m) were tested at two vessel speeds (20 and 38 knots) and one modal period (8.5 s) only. This plan gave a total of twenty-two conditions, the parameters which are summarised in Table 2.

In order to establish a comparison between different conditions, the encountered modal wave frequency was estimated from the wave spectrum modal period and ship speed. The modal encountered wave frequency was estimated by calculating the wave celerity, c, of a group of waves with a period of the modal period of the spectrum. In deep water the wave celerity is defined as:

$$c = \frac{T_0 g}{2\pi}. \qquad \text{eq. 3.1}$$

Here T_0 is the period of the wave. The deep water assumption was found to be valid for model scale modal periods of 1 and 1.3 s, given a water depth of 1.5 m. However the 1.5 s modal period conditions were in the transitional region. Therefore the dominant wave length was estimated by equation 3.2, [9]:

$$\lambda \approx \frac{gT_0}{2\pi}\sqrt{\tanh\left(\frac{4\pi^2}{T_0^2}\frac{d}{g}\right)}, \qquad \text{eq. 3.2}$$

where d is the water depth (1.5 m), and the corresponding wave celerity was determined by equation 3.3. This method is accurate to within about five percent [9]. The wave length determined by eq. 3.2 for T_0 = 1.5 s was found to be within 1% of the deep water equivalent. Therefore the conditions can be assumed to be deep water.

$$c = \frac{gT_0}{2\pi}\tanh\left(\frac{2\pi d}{\lambda}\right) \qquad \text{eq. 3.3}$$

The modal encountered wave frequency can then be determined by

$$f_e = \frac{U + c}{cT_0}. \qquad \text{eq. 3.4}$$

Here U is the forward speed of the vessel. The encountered wave frequency was then made non-dimensional by applying

$$\omega_e^* = 2\pi f_e \sqrt{L/g}. \qquad \text{eq. 3.5}$$

Here, L is the length of the vessel. Table 3 summarises the test conditions and the corresponding calculated dimensionless encountered wave frequencies.

Table 3: Test conditions and the corresponding dimensionless encounter frequency ω_e^*.

ω_e^*	Model scale T_0 (s)	Model scale U (m/s)	Full scale T_0 (s)	Full scale U (kn)
3.49	1.5	1.54	10	20
4.04	1.5	2.15	10	28
4.28	1.3	1.54	8.5	20
4.73	1.5	2.92	10	38
5.02	1.3	2.15	8.5	28
5.91	1.3	2.92	8.5	38
6.28	1.0	1.54	7.0	20
7.54	1.0	2.15	7.0	28
9.04	1.0	2.92	7.0	38

4. RESULTS AND DISCUSSION

4.1 SLAM IDENTIFICATION

Slam events have been previously identified by defining a threshold rate of change of load (or stress in the case of full scale measurements) and a threshold load which can be thought as a ‘minimum’ slam load. In previous model tests in irregular seas, the slam criteria were chosen as a threshold of 10 N and a minimum rate of change of load of 5,000 N/s [4]. A similar method was employed by Thomas et al. [10] when investigating full scale data from stain gauges. In the present tests only a rate criterion was defined in order to capture small slam events.

Although slam events can be identified by the centrebow strain gauge data, it was found that the pressure data provided much clearer slam indication. This meant that a slam criterion was not necessary; instead local pressure peaks provided slam event flags. A semi-automated process was established, where the pressure records from a key pressure transducer were scanned by a peak detection algorithm and the majority of slam events were thus identified. Each run was manually examined to ensure that no events were missed by the algorithm and any events that have been mistakenly identified were deleted. A total of 2,098 slam events were identified in the 22 test conditions.

In order to adequately capture the peak centrebow surface pressure during a slam event, a study was conducted into the influence of the DAQ sample rate on the peak measured pressures. Firstly several calm water runs were conducted and the pressure signals were examined to ensure that there were no unexpected spikes that could be misidentified as slam events. The model was then tested in large regular waves, where slamming was known to occur. Runs in this condition were repeated several times with the DAQ sample rate changed in steps from 500 Hz to 5 kHz. Pressure peaks were the identified and the maximum, minimum and average measured pressures for each sample rate were compared. Significant variations in peak pressures were observed between runs at all sample frequencies; therefore it was decided to sample at the highest frequency of 5 kHz in order to maximise resolution of the pressure peaks.

The pressure transducer closest to the centrebow truncation (CBT) was used as the reference location as it has been found from previous studies in regular waves that the location of maximum load tends to occur in this vicinity [5].

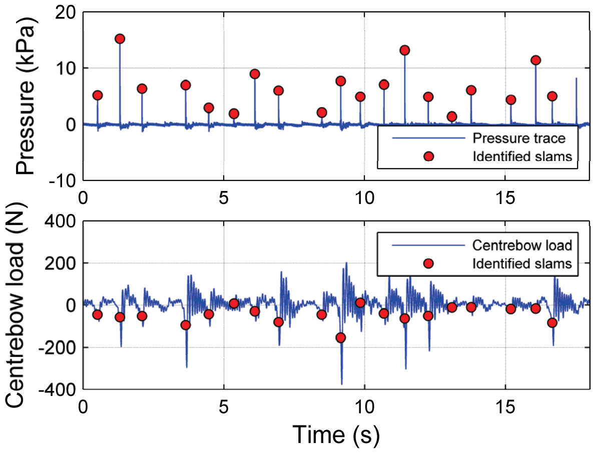

Figure 3: Pressure and centrebow load trace with identified slams highlighted with circles (negative load is up on the centrebow). T_0 = 1.5 s, $H_{1/3}$ = 78.1 mm, U = 2.15 m/s.

Figure 3 shows time traces of the pressure and centrebow load data from a typical test run. Slams are easily identifiable from the pressure trace alone: circles are used to highlight the identified slams and they are reproduced on the centrebow load trace below. Negative centrebow load is defined as 'up'. The maximum pressure is recorded just before the maximum centrebow load is measured. The time when the maximum pressure was recorded on the transducer in line with the CBT has been defined as the slam instant in this work. This is an arbitrary definition used primarily for slam identification. The actual slam instant could vary from this time, particularly if the slam was located away from the centrebow truncation where there would be a time delay between the actual slam occurrence and the measured pressure peak at the centrebow truncation.

The total number of slams for each condition has been summarised in Table 4 In order to produce a meaningful sample of slam events as many slam events were recorded per condition as possible. The duration of each condition (scaled to full scale) is shown in Table 5. A thorough investigation into the slam occurrence rates of the wave-piercing catamaran from this data is presented in French et al. [11].

Table 4: Number of slam events measured for each condition.

	Significant wave height			
ω_e^*	2.5 m	3.0 m	3.5 m	4.0 m
3.49	-	-	83	82
4.04	-	-	110	100
4.28	66	104	131	171
4.73	-	-	90	66
5.02	-	-	132	137
5.91	43	71	98	86
6.28	-	-	97	83
7.54	-	-	101	106
9.04	-	-	83	58

Table 5: Full scale duration for each condition.

	Duration (full scale, minutes)			
ω_e^*	2.5 m	3.0 m	3.5 m	4.0 m
3.49	-	-	23.2	17.4
4.04	-	-	16.1	14.1
4.28	23.2	23.2	23.2	23.2
4.73	-	-	10.7	9.4
5.02	-	-	16.1	16.1
5.91	9.4	10.7	10.7	9.4
6.28	-	-	26.1	20.3
7.54	-	-	16.1	14.1
9.04	-	-	10.7	8.0

4.2 WAVE LOADS

From a design perspective, it is important to consider the maximum load the vessel structure will be likely be exposed to. However, the aim of this analysis was to isolate the slam load from the global wave loads. The resulting slam load component can then be used in the structural design of future vessels by being applied to a dynamic finite element model.

The measured load is considered to consist of three separate load components: inertial, global wave and slam loads. A diagram showing the different load components can be seen in Figure 4. Slam forces are induced by water impact on the centrebow archway and wet deck, low frequency global forces are due to the immersion of the centrebow (a cyclic load that coincides with the encountered wave frequency) and the inertial force is proportional to the acceleration of the centrebow segment.

Inertial loads on the centrebow were estimated by applying Newton's Second Law of Motion $F = ma$, where the mass m relates to the mass of the centrebow segment and all other associated material on the centrebow (the transverse beams, aluminium nuts and bolts, pressure transducers, cable masses etc.) and the acceleration a is the acceleration of the centre of mass of the centrebow.

Since no channels were available for acceleration measurements during the tests presented here, the acceleration of the bow was estimated by assuming the model to be a rigid body and determining accelerations from the motions data. To test the suitability of this method, test data from Amin [12] (when an accelerometer was installed on the centrebow of the same model) were examined. The condition chosen consisted of a wave height of 120 mm (regular waves) and wave frequency of 0.65 Hz. The model speed was 1.53 m/s, giving a dimensionless encounter frequency of 3.27.

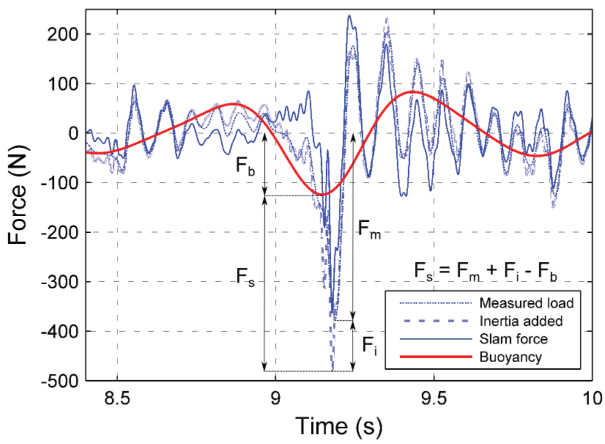

Figure 4: Measured centrebow load decomposed into force components: slam force, low frequency global load and inertial force. Structural vibrations, or whipping, of the model can be seen after the slam at 9.2s.

Bow accelerations were calculated from the LVDT signals and compared with those measured from the accelerometer, as shown in Figure 5. The accelerations derived from the global motions of the model are seen to correlate well with the accelerations measured by the accelerometer (correlation coefficient, r = 0.854, at the 95% confidence interval), thus providing confidence in using the LVDT signal to determine the acceleration on the centrebow for this set of experiments. The moderate oscillations found in the LVDT trace can be attributed to vibrations in the tow posts recorded by the LVDTs or the motions of the wetdeck segment of the model.

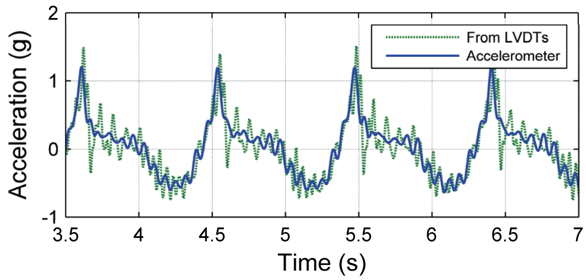

Figure 5: Comparison between accelerations measured from accelerometer and derived from LVDT signals (from [12], Run 22, 120 mm wave height, 0.65 Hz wave frequency, 1.53 m/s ω_e^* 3.27)).

Low frequency global loads measured by the centrebow segment strain gauges are induced by the centrebow entering and leaving the water and so are considered to have similar loading frequencies as the encountered wave frequency. A Butterworth low-pass filter was used to isolate the wave components associated with global wave loading. These loads could then be subtracted from the total centrebow load to isolate the slam load. An investigation into the sensitivity of the cut-off frequency on the resulting slam load was undertaken to determine the appropriate cut-off frequency. The cut-off frequency is defined as the frequency where half the signal power is attenuated (-3dB). Since a series of sea conditions with varying modal periods and vessel speeds and thus encounter frequencies was tested, the cut-off frequency was defined as a multiple of the encountered modal frequency for a given condition. The ideal cut-off frequency to isolate the global wave load without attenuating the higher frequency slam load was found to be twice the encountered wave frequency.

4.3 RELATIVE VERTICAL VELOCITY AND CENTREBOW SLAM LOAD

The vertical velocity of the model and wave surface elevation at the centrebow truncation was calculated by numerically differentiating the displacement time trace of the vessel and wave probe located in line with the centrebow truncation (WP1 in Figure 1) respectively. The influence of forward speed of the towing tank carriage on the wave surface vertical velocity was neglected in this process. The relative vertical velocity between the vessel and wave was then obtained. Positive relative vertical velocity is defined as the vessel and wave moving towards one another.

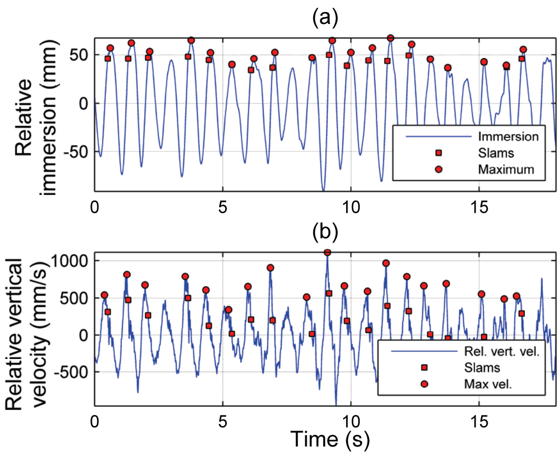

Figure 6: (a) Relative immersion of the catamaran model at the CBT. (b) Relative vertical velocity at the CBT. Identified slam events are highlighted with squares, and local maxima are highlighted with circles. T_0 = 1.5 s, $H_{1/3}$ = 78.1 mm, U = 2.15 m/s.

The maximum relative vertical velocity of the hull to the water surface prior to a slam was calculated for each identified slam event. Figure 6 shows the relative immersion and vertical velocity for a sample run. The slam instants (time when the maximum pressure at the CBT was measured) are shown by filled squares and the maximum immersion and relative vertical velocity are highlighted by circles. Slams are generally found to occur prior to the maximum immersion followed by a rapid acceleration in the direction opposite to the current motion. Figure 7 shows box plots of the distributions of relative vertical velocity at the recorded slam instant for each test condition. The box plot is a useful tool to compare distributions as it lays them side by side, as opposed to viewing the probability density function (pdf) as a histogram or frequency polygon. The top of the box represents the upper quartile (Q_3, or the 75th percentile) and the bottom of the box shows the lower quartile (Q_1, 25th percentile). The box itself encompasses the interquartile range (IQR), hence 50% of the measurements fall within the box. The middle line, dividing the box in two, is the median value of the data set. Therefore visual comparisons of different data sets can be made directly by the box plots. Whiskers (the dashed lines) extend above and below the boxes to enclose the lowest and highest values within 1.5 of the interquartile range (i.e. the 'height' of the box). Data outside of this range is marked individually can be considered as outliers. A number of outliers are evident in Figure 7, particularly negative relative velocities for the 78.1 mm significant wave height conditions.

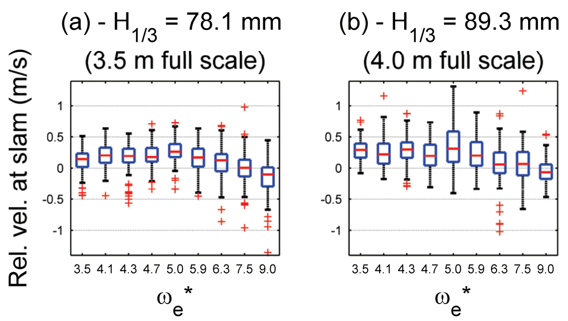

Figure 7: Box plots describing the distributions of relative vertical velocity at the maximum pressure instant against dimensionless encounter frequency. (a) $H_{1/3}$ = 78.1 mm (3.5 m full scale). (b) $H_{1/3}$ = 89.3 mm (4.0 m full scale).

The median velocity at the slam instant tends to be greater than zero for dimensionless encounter frequencies less than 6.3. This can be clearly seen in Figure 7. The higher encountered wave frequencies are more likely to result in negative relative vertical velocities at the slam instant. The IQR for ω_e^* = 9.04, $H_{1/3}$ = 78.1 mm/3.5 m is almost entirely negative (greater than 50% of the recorded slams are negative), suggesting that slams tend to be located away from the CBT at these higher wave encounter frequencies. This phenomenon has been previously observed during a shorter preliminary model test programme in irregular seas: the slam location tended to move aft with increasing forward speed [4].

Figure 8 shows the distributions of maximum relative vertical velocity prior to the slam event. The maximum relative velocity prior to a slam event is greater than 0.5 m/s for the majority of recorded slam events for all conditions. Maximum relative velocities prior to slamming tend to increase with the dimensionless wave encounter frequency and decrease slightly for the higher encounter frequencies. This trend is also seen in the centrebow slam magnitude distributions shown in Figure 9 and the heave motion response of the vessel in waves [13]. The slam magnitudes are relatively mild for low and high encounter periods, when vessel motions are small. However numerous outliers have been measured up to four times the median in most conditions, confirming that although motions (and thus velocities) may be small in general, significant slam events may still occur. It is also evident from Figure 9 that the median slam magnitudes for the 4.0 m sea conditions are greater than the corresponding 3.5 m conditions. Even though slam events tend to be more severe in the larger wave conditions, the largest slam recorded during these tests was recorded in a 3.5 m condition (ω_e^* = 5.91, T_0 = 8.5 s, U = 38 kn, full scale). This emphasises the importance of adopting a statistical approach when investigating slamming in irregular waves, and entices further research into understanding the largest (likely) slam event in a given condition.

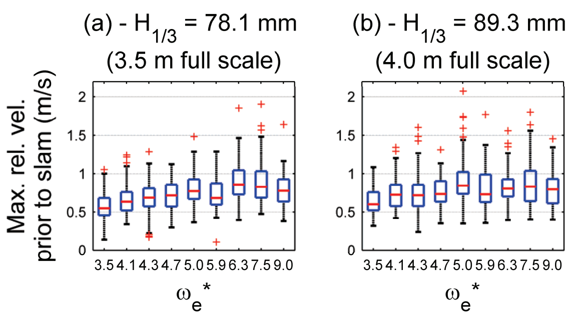

Figure 8: Box plots describing the distributions of maximum relative vertical velocity prior to slamming against dimensionless encounter frequency. (a) $H_{1/3}$ = 78.1 mm (3.5 m full scale). (b) $H_{1/3}$ = 89.3 mm (4.0 m full scale).

Interestingly, at the high encounter frequencies (ω_e^*>6.3), slam loads are relatively mild but the maximum relative vertical velocity prior to slamming distributions are similar to those of more severe slamming conditions, suggesting that other factors contribute to the resulting slam loads.

The correlation between relative vertical velocity and centrebow slam magnitude are examined in the scatter plots shown in Figures 10 and 11. The relative vertical velocities prior to slam are shown in Figure 10 on the x-axis and the relative velocity at the slam event time is plotted in Figure 11. Data is grouped by Froude number. Whilst there is a weak relationship between the peak relative vertical velocity and slam load, there appears to be a clearer trend between the relative vertical velocity at slam and slam load. This observation is supported by a correlation coefficient, r= 0.58, for relative velocity at the recorded slam instant compared to a correlation coefficient of 0.45 for the maximum relative velocity prior to the slam event. This implies that the relative vertical velocity at the time of impact is a somewhat better indicator of slam magnitude than the peak relative vertical velocity prior to the slam. The relation between relative vertical velocity at impact and the maximum prior to impact was investigated, but poor correlation was identified (r = 0.19). However it is noted that the velocity at the times peak pressures are measured could be sensitive to the physical location of the pressure transducer.

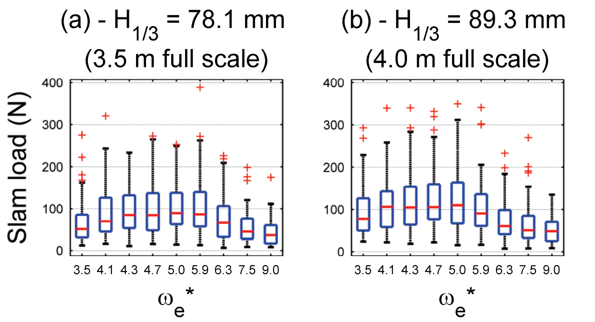

Figure 9: Box plots describing the distributions of slam load against dimensionless encounter frequency. (a) $H_{1/3}$ = 78.1 mm (3.5 m full scale). (b) $H_{1/3}$ = 89.3 mm (4.0 m full scale), (Figure 15 from [11]).

If the transducer is mounted away from the actual slam location, then there will be a delay between the time when the slam event occurs and when the pressure transducer records a pressure spike. That being said, the seemingly better correlation between relative vertical velocity when the pressure peak is measured and slam load may simply be coincidental.

It is apparent from these plots that for a particular relative vertical velocity (either the maximum prior or the velocity at the recorded event), there are a range of possible slam force magnitudes. Previous investigations have already observed a weak association between velocity and slam load [4]. Therefore the slam load cannot be determined by relative vertical velocity alone.

4.4 CENTREBOW IMMERSION AND ARCHWAY WAVE ELEVATIONS

The centrebow truncation point was chosen as the reference location to measure bow immersion. This location was selected as it was observed from slamming investigations in regular seas that the onset of slamming occurred when the water displaced in the archway due to bow immersion at this point approximately equalled the two dimensional area of the arch tunnel [5]. This observation was defined as the 2D filling height [5], shown in Figure 12. This parameter is based on the observation that slam events appeared to occur prior to the archway filling completely with water. For this model configuration, the 2D filling height is approximately 50mm above the calm water line at the CBT. Since the maximum centrebow immersion does not coincide with the time when surface pressures are greatest, as seen in Figure 6, both the centrebow immersion and the maximum immersion after the slam event were measured and analysed.

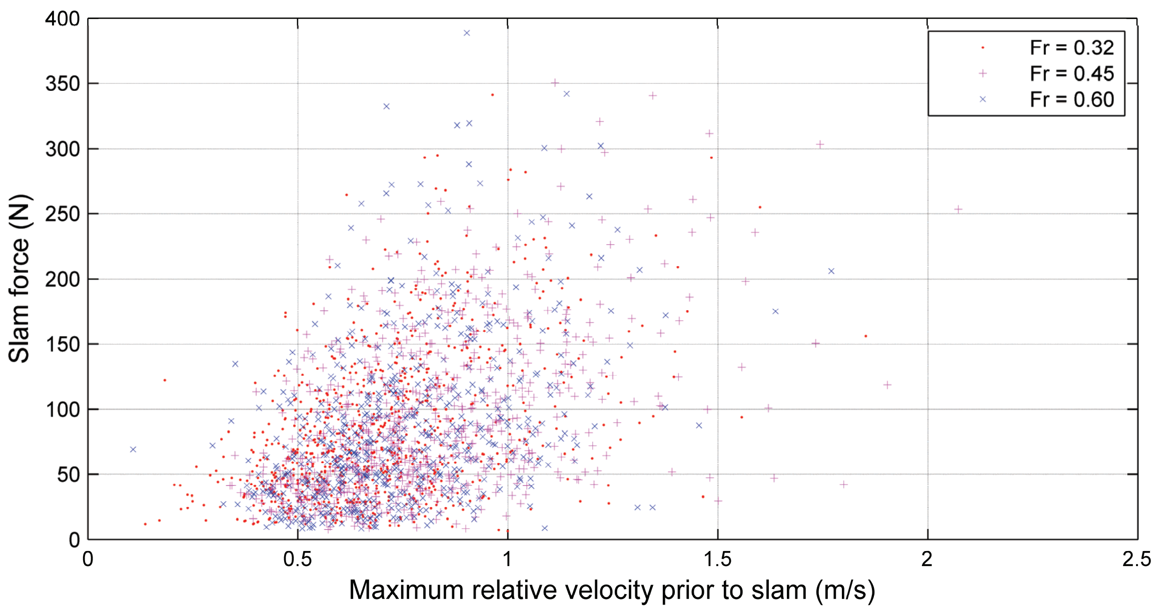

Figure 10: Maximum relative velocity prior to slam event against slam load. Data grouped by Froude number.

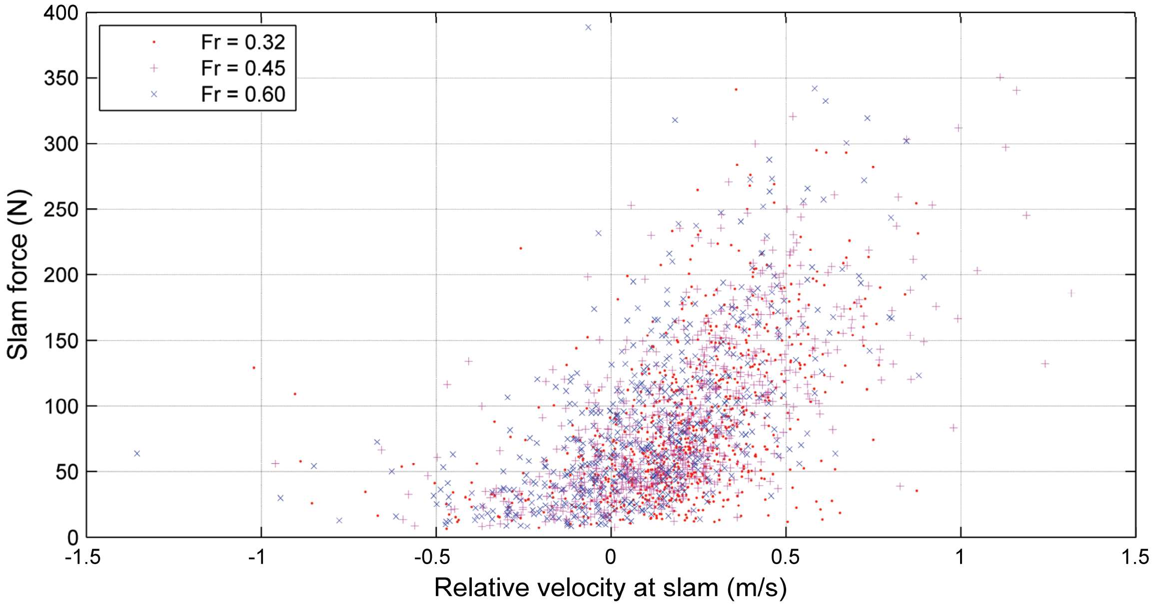

Figure 11: Relative velocity when slam occurred against slam load. Data grouped by Froude number.

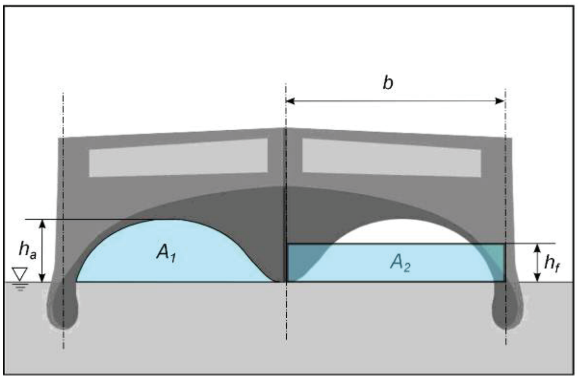

Figure 12: Definition of the 2D filling height. $A_1 = A_2$, h_f is the 2D filling height.

Slams at higher encountered frequencies $\omega_e^* > 6.3$ are found to differ from 'normal' slams: they are characterised by a small, often negative, relative vertical velocity at the CBT when the maximum pressure is recorded, small immersion at the CBT and are located further aft on the centrebow segment than at other encountered frequencies. Slam loads at these higher encountered wave frequencies are also generally lower than other conditions. It can be concluded that these types of slams are primarily the result of relatively shorter wave impacts on the vessel, with little vessel motion contributing to the relative motions of ship and wave as opposed to slams at lower encounter frequencies where the vessel impacts on the wave, with vessel motions contributing significantly to the relative motions of the ship and wave.

Figure 13(a) shows the immersion of the centrebow truncation at the time of greatest pressure for significant wave heights of 3.5 m (full scale), whereas Figure 13(b) shows the distributions for $H_{1/3}$ = 4.0 m. Data is grouped by dimensionless encounter frequency. Similarly, Figure 14 shows the distributions of maximum immersion after the slam event. The maximum arch height (h_a) relative to the calm water level (approximately 80 mm at the centrebow truncation) and the 2D filling height (h_f)are included in these figures. It can be seen that almost all recorded slam events occur well before the bow is immersed sufficiently to bring the maximum archway level to the encountered water level. Also, from these distributions the 2D filling height cannot be declared as an exact threshold condition for slam occurrence predictions as slam events tend to occur around the 2D filling height. From Figure 13 it can be seen that the majority of slams occur at immersions less than the 2D filling height, with the exceptions of ω_e^* = 6.28.

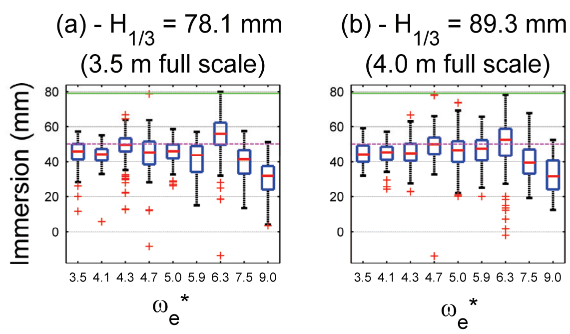

Figure 13: Distributions of immersion at the centrebow truncation against dimensionless encounter frequency. (a) $H_{1/3}$ = 78.1 mm (3.5 m full scale). (b) $H_{1/3}$ = 89.3 mm (4.0 m full scale). The maximum arch height (solid line) and the 2D filling height (dotted line) are also shown.

Also apparent in these plots is that the slam events almost always occur and are concluded at immersions less than the maximum arch height. However in Figure 14 we see that the maximum immersion has exceeded the maximum arch height on several occasions, particularly in the mid-range encounter frequencies and larger wave height conditions, where vessel motions are the greatest.

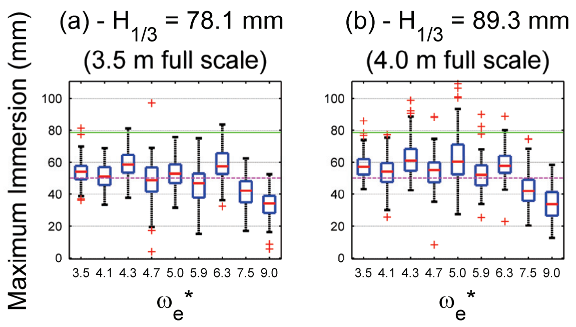

Figure 14: Distributions of maximum immersion at the centrebow truncation against dimensionless encounter frequency. (a) $H_{1/3}$ = 78.1 mm (3.5 m full scale). (b) $H_{1/3}$ = 89.3 mm (4.0 m full scale). The maximum arch height (solid line) and the 2D filling height (dotted line) are also shown.

Wave elevations under the archway were measured using three wave probes. A fourth probe was located on the centre line of the model, 120 mm aft of the centrebow truncation. A time trace of the different wave elevations under the bow archway and the calculated centrebow immersion at the CBT is shown in Figure 15. Figure 15(a) shows relative immersion at the centrebow truncation (calculated by taking the difference between the displacement at the CBT and the wave elevation measured by a wave probe located in plane but transversely offset from the CBT). Slam events are shown by circles. Figure 15(b), (c) and (d) show wave elevations between the demihulls. The wave probes occasionally come completely out of the water; this is most evident by the flat bottoms in Figure 15(b) where the probes emerge on almost every wave. This probe is mounted the furthest forward on the bow, and thus it is the highest relative to the calm water line. Wave probe emergence has been captured in several still camera photos; Figure 16 shows one instance where wave probes 2 and 3 (120mm forward and in plane with the centrebow truncation respectively) have completely emerged from the water.

Figure 15 also shows the measured wave elevations within the archway tunnel at the identified slam events. The maximum archway height (at the centrebow truncation) is shown in the plots with a solid line. The archway does not appear to be completely filled when a slam occurs and the events always occur prior to the maximum recorded relative wave height. This could happen if the slam occurred at a different location from those where the wave probes are mounted. Figure 15(c) is of particular interest, because this is the reference point for the 2D filling height. It attempts to account for water displaced by the centrebow when the bow is immersed. For this model configuration, the 2D filling height is approximately 50mm from the calm water line at the CBT. For the condition shown in Figure 15(c), the majority of slam events occur when the recorded wave elevation is between 40-50 mm, close to the 2D filling height parameter.

5. CONCLUSIONS

Slam parameters and characteristics were identified by testing a hydroelastic scale model of a 112m INCAT Tasmania catamaran. A total of 2,098 slam events were identified over 22 different conditions; each condition containing about 80 to 100 slam events. Centrebow slam loads were determined by analysing strain gauge signals mounted on the centrebow transverse beams.

A statistical approach was adopted when investigating slam characteristics because it is inappropriate to compare individual slams in irregular waves. Distributions of the gathered samples of slamming behaviour in each sea condition were compared instead. This approach gives an indication of not only typical observations but also the likelihood of extreme events.

The encountered wave frequency is an important parameter with regard to centrebow slamming. Slam loads, although scattered, tends to follow ship motion trends and large motions result in large slams. The distribution of slam magnitudes showed that the median is a function of significant wave height and encountered wave frequency. However many outliers were detected and extreme slam events up to four times the median were recorded for most conditions.

The relative vertical velocity between the wave and vessel was another parameter investigated during model slam testing. The maximum vertical velocity prior to a slam event and the velocity when a slam event occurred were determined. The median velocity at the slam instant tends to be greater than zero for moderate to low dimensionless encounter frequencies. At high wave encounter frequencies more negative relative velocities are measured, suggesting that the slam location is then further away from the CBT.

Maximum relative vertical velocities tended to increase with wave encounter frequency. At high encounter frequencies the maximum relative velocities prior to the slam event remain large, whereas the distributions of slam load magnitudes are relative mild. This shows that the maximum relative vertical velocity prior to the slam event may not be a reliable slam magnitude predictor.

The 2D filling height, previously defined from regular sea tests, was considered and compared with centrebow immersions during slamming. Slams were found to start before the immersion of the centrebow reached the maximum arch height, and were also generally concluded before the maximum arch height was reached, with the exception of the 89.3 mm model scale (4.0 m full scale) significant wave height conditions. Some extreme slams in these conditions resulted in immersions up to twice the maximum arch height at the centrebow truncation. Scatter of the immersion data showed that the 2D filling height, at which displaced water would fill the arched cross section calculated on a simple two dimensional basis, cannot be used as an exact threshold for centrebow slamming. However, the 2D filling height parameter does provide a useful indicator for understanding the onset conditions for slamming and thus for the prediction of slam occurrences.

The implications of this work are that scale model tests in irregular seas are valuable in ship design. Statistical methods need to be adopted as individual slams in irregular waves are inherently diverse. However, the statistics, or distributions, of slamming characteristics in different sea conditions can be compared. With more data the vessel designer can define a design slam load by amalgamating the slam distributions from a series of sea conditions weighted by the expected exposure time, then determining the design load based on the probability of exceedance over a given time.

6. ACKNOWLEDGEMENTS

This work has been partly supported by INCAT Tasmania, Revolution Design Pty. Ltd. and the Australian Research Council. The authors would like to acknowledge the help of their colleagues at the Australian Maritime College, the University of Tasmania, Revolution Design Pty. Ltd. and INCAT Tasmania.

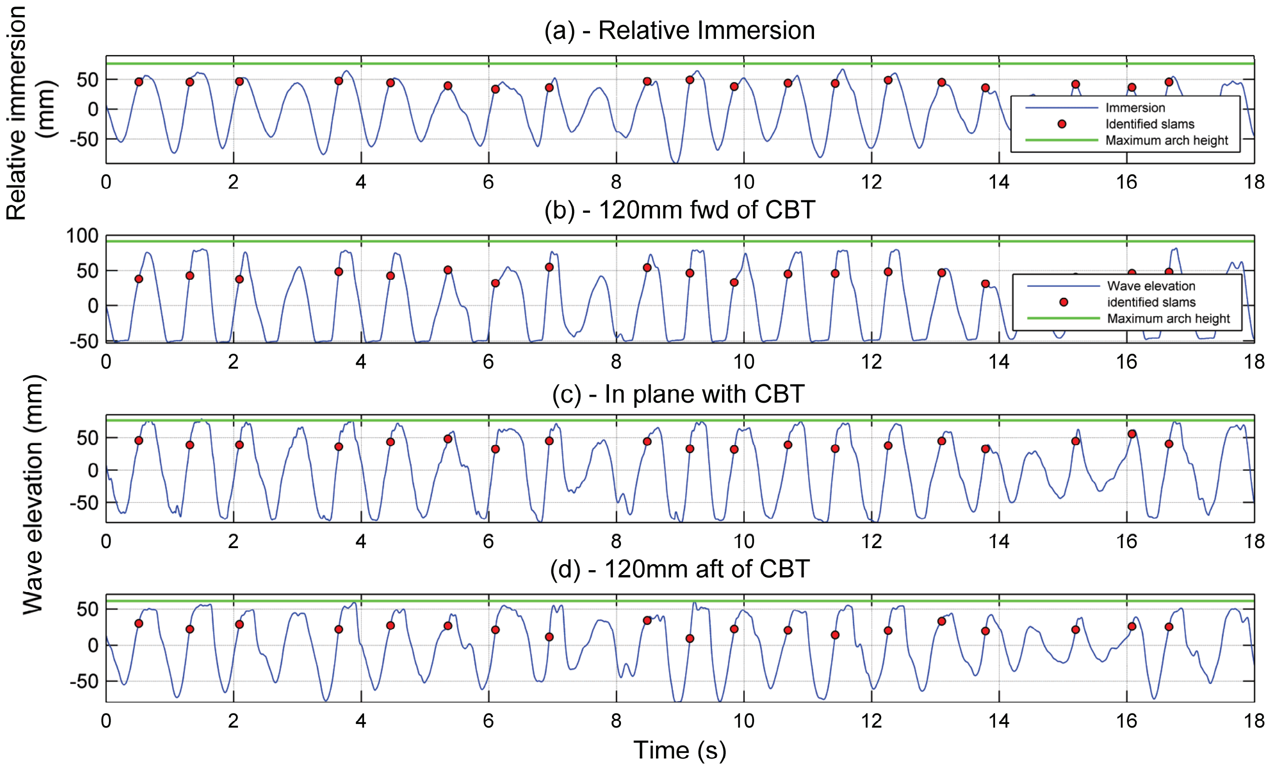

Figure 15: Wave elevations for one run. Identified slam events are shown with circles. (a) Relative immersion at the CBT. (b) Surface elevation 120 mm forward of the CBT. (c) At the CBT. (d) 120 mm aft of the CBT. Wave probes (b), (c) and (d) are located in line with the maximum archway.T_0 = 1.5 s, $H_{1/3}$ = 78.1 mm, U = 2.15 m/s.

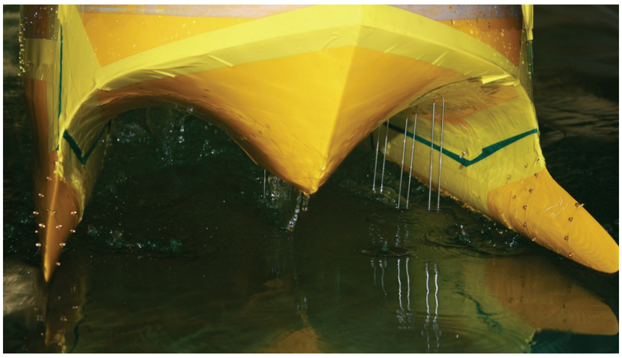

Figure 16: Still photograph of the centrebow taken during experimental tests. The wave-piercer bows have completely emerged from the water along with two boat mounted wave probes (WP2 and WP3). WP5, mounted in the centreline of the model, 120mm aft of the centrebow truncation, can also be seen.

7. REFERENCES

1. DAVIS, M.R., LAVROFF, J., FRENCH, B., THOMAS, G.A., HOLLOWAY, D.S. and ROBERTS, T.R., The Prediction of Wetdeck Slam Loads on High-Speed Catamarans, *International Maritime Exposition, PACIFIC 2010*, Sydney, January 2010.
2. MATSUBARA, S., THOMAS, G., DAVIS, M., HOLLOWAY, D. and ROBERTS, T., Influence of Centrebow on Motions and Loads of High-Speed Catamarans, *Proceedings of the 11th International Conference on Fast Sea Transportation (FAST 2011)*, 26-29 September 2011, Honolulu, Hawaii, pp. 661-668, 2011.
3. LAVROFF, J., DAVIS, M., HOLLOWAY, D. and THOMAS, G, Determination of Wave Slamming Loads on High-Speed Catamarans by Hydroelastic Segmented Model Experiments*, International Journal of Maritime Engineering*, Vol. 153 (A3) pp. 185-197, 2011.
4. THOMAS, G., WINKLER, S., DAVIS, M., HOLLOWAY, D., MATSUBARA, S., LAVROFF, J. and FRENCH, B., Slam Events of High-Speed Catamarans in Irregular Waves. *Journal of Marine Science and Technology*. Vol. 16, pp. 8-21, 2011.
5. LAVROFF, J., The Slamming and Whipping Vibratory Response of a Hydroelastic Segmented Catamaran Model. *School of Engineering, PhD Thesis*. University of Tasmania, 2009.
6. WHELAN, J.R., Wetdeck Slamming of High-Speed Catamarans with a Centrebow, *School of Engineering PhD Thesis*, University of Tasmania, 2004.
7. DAVIS, M.R., WHELAN, J.R. and THOMAS, G.A., Computational Modeling of Wet Deck Slam Loads with Reference to Sea Trials. *FAST2007 Ninth International Conference on Fast Sea Transportation*, Shanghai, China, 2007.
8. LLOYD, A., *Seakeeping: Ship Behaviour in Rough Weather*, Ellis Horwood, 1989.
9. UNITED STATES ARMY CORPS OF ENGINEERS, COASTAL ENGINEERING RESEARCH CENTER (U.S.), *Shore Protection Manual, Volume 1*, 1984.
10. THOMAS, G., DAVIS M.R., HOLLOWAY D.S., WATSON, N.L. and ROBERTS, T.J., Slamming Response of a Large High-Speed Wave-Piercer Catamaran. *Marine Technology*. Vol. 40, pp. 126-40, 2003.
11. FRENCH, B., THOMAS, G. and DAVIS, M., Slam Occurrences and Loads of a High-Speed Wave Piercer Catamaran in Irregular Seas, *Proceedings of the Institution of Mechanical Engineers, Part M: Journal of Engineering for the Maritime Environment*, 2013. (In Press).
12. AMIN, W., Non-Linear Unsteady Wave Loads on Large High-Speed Wave Piercing Catamarans. *School of Engineering PhD Thesis*. University of Tasmania, 2009.
13. FRENCH B., THOMAS G., DAVIS M. and HOLLOWAY, D., A High Froude Number Time-Domain Strip Theory for Ship Motion Predictions in Irregular Waves. *18th Australasian Fluid Mechanics Conference.* Launceston, Australia, 2012.

